ORIGINAL PAPER

DOI: http://dx.doi.org/10.15403/jgld-2834

Elevated *TUBA1A* Might Indicate the Clinical Outcomes of Patients with Gastric Cancer, Being Associated with the Infiltration of Macrophages in the Tumor Immune Microenvironment

Dazhi Wang[1,2], Zheng Jiao[1], Yinghui Ji[3], Shuyu Zhang[1]

1) Center for Precision Cancer Medicine, Clinical Oncology Pharmacist Training bases (National Health Commission), Department of Pharmacy, Qingdao Municipal Hospital, Shandong University, Qingdao;
2) Key Laboratory of Chemical Biology (Ministry of Education), Department of Medicinal Chemistry, School of Pharmaceutical Sciences, Cheeloo College of Medicine, Shandong University, Jinan;
3) Clinical Oncology Pharmacist Group, Affiliated Hospital of Weifang Medical University, Weifang, China

Address for correspondence:
Dazhi Wang
Center for Precision Cancer Medicine, Clinical Oncology Pharmacist Training bases (National Health Commission), Department of Pharmacy, Qingdao Municipal Hospital, Shandong University, Donghai Road 5, Qingdao, Shandong 266071, China
dazhi_wang@mail.sdu.edu.cn

Received: 21.07.2020
Accepted: 19.10.2020

ABSTRACT

Background & Aims: TUBA1A belongs to the tubulin superfamily, and its role in gastric cancer (GC) remains unclear. This study assessed the expression and effect of *TUBA1A* in GC, as well as its association with survival and clinicopathological features. Gene set enrichment analysis (GSEA) results revealed that high *TUBA1A* expression was associated with multiple pathways, including those that contributed to the infiltration of macrophages in the tumor microenvironment. Since increased infiltration of macrophages can lead to oxaliplatin resistance, we analyzed the association between *TUBA1A*, the infiltration of macrophages to the tumor microenvironment, and the inhibitory concentration 50% (IC50) of oxaliplatin. In addition, we analyzed the possible epigenetic regulation mechanism.

Methods: A total of 1,881 samples, including 1,618 patients with GC and 263 normal samples, were examined. The associations between clinicopathological features and *TUBA1A* were assessed by chi-square test, survival was assessed by Kaplan-Meier analysis, and gene set enrichment analysis (GSEA) was performed to explore the potential mechanisms. The associations between *TUBA1A* and immune infiltration of M0-, M1-, and M2-polarized macrophages were examined by applying deconvolution's quantification and Pearson's correlation analysis. The association of *TUBA1A* with the IC50 of oxaliplatin was analyzed by Pearson correlation test. The mechanisms of *TUBA1A* dysregulation were studied by analyzing methylation data. A single-cell *TUBA1A* mRNA expression map of the stomach was drawn from the analysis of stomach single-cell RNA sequencing data that included more than 13,000 single cells of 17 stomach cell types.

Results: *TUBA1A* expression was elevated in GC ($p<0.01$) and indicated poorer overall survival ($p<0.001$), first progression survival ($p<0.001$), and post-progression survival ($p<0.01$). High *TUBA1A* expression was significantly correlated with more aggressive clinicopathological features of GC patients ($p<0.001$). Elevated *TUBA1A* contributes to the infiltration of macrophages to the tumor microenvironment ($p<0.001$) and increased the IC50 of oxaliplatin in vitro ($p<0.05$), while hypomethylation was shown to contribute to the upregulation of *TUBA1A* ($p<0.05$).

Conclusions: *TUBA1A* might be a potential prognostic marker and therapeutic target in GC. *TUBA1A* is significantly associated with the infiltration of M2-polarized macrophages in GC, and the IC50 of oxaliplatin. Hypomethylation contributes to the upregulation of *TUBA1A* in GC.

Key words: tumor biomarkers – poor prognosis – *TUBA1A* – gastric carcinoma – tumor immune microenvironment.

Abbreviations: CSF-1: colony stimulating factor 1; CCL2: C-C motif chemokine ligand 2; Cor: Pearson's correlation coefficient; CXCL12: C-X-C motif chemokine ligand 12; CX3CL1: C-X3-C motif chemokine ligand 1; ES: enrichment score; FDA: false discovery rates; FTO: the fat mass- and obesity-associated protein; GC: gastric cancer; GDSC: Genomics of Drug Sensitivity in Cancer; GEO: Gene Expression Omnibus; GEPIA: the Gene Expression Profiling Interactive Analysis; GSE: Gene Expression Omnibus Series; GSEA: gene set enrichment analysis; GSK3: glycogen synthase kinase3; GSVA: Gene Set Variation Analysis; GTEx: the Genotype-Tissue Expression; HDAC: histone deacetylase; HPA: the Human Protein Atlas; IC50: inhibitory concentration 50%; IHC: immunohistochemical; KM: Kaplan Meier; LM22: 22 leukocyte subsets; MCA: the Mouse Cell Atlas; mTOR: mammalian target of rapamycin; STAD: stomach adenocarcinoma; TAMs: tumor-associated macrophages; ssGSEA: single sample gene set enrichment analysis; TCGA: the Cancer Genome Atlas; UICC: Union for International Cancer Control; VEGFC: vascular endothelial growth factor C.

INTRODUCTION

Gastric cancer (GC) is the second leading cause of cancer-related mortality worldwide, and the most common malignant tumor in the digestive system; however, the pathogenesis of GC remains unclear. *TUBA1A*, which encodes the tubulin alpha-1A chain, was the first tubulin gene to be associated with brain malformations [1, 2]. *TUBA1A* belongs to the tubulin superfamily, and participates in numerous cellular processes, including intracellular transport, cell division, cell movement, and neuronal migration [3-5]. Recently, *TUBA1A* was found to be upregulated in breast cancer tissues [6]. The role of *TUBA1A* in GC is unknown.

The tumor immune microenvironment plays a critical role in tumor pathological processes [7]. In tumor microenvironment, macrophages can be phenotypically polarized by the microenvironment to M1 macrophages (classically activated macrophages) or M2 macrophages (alternatively activated macrophages); unactivated macrophages is defined as M0 macrophages. In malignant tumors, M2-polarized tumor-associated macrophages (TAMs) are important tumor-infiltrating immune cells that have tumor-promoting functions [8-10]. In recent study, histone deacetylase (HDAC) pathway, glycogen synthase kinase3 (GSK3) pathway, mammalian target of rapamycin (mTOR) pathway, and P38MAPK pathway are known to contribute to macrophage polarization and infiltration of M2-polarized TAMs [11-14]. However, no study has examined the association between *TUBA1A* and the infiltration of M2-polarized TAMs in the gastric tumor microenvironment.

Oxaliplatin is a common treatment in GC [15-17]; however, its efficacy is limited due to resistance, which is mediated by changes in the tumor immune microenvironment [18, 19].

We performed a comprehensive analysis of the expression of *TUBA1A* in GC and evaluated its association with survival and clinicopathological features. We also aimed to determine the possible epigenetic regulation mechanism underlying the dysregulation of *TUBA1A*. We investigated the influence of *TUBA1A* on oxaliplatin by analyzing the correlation between *TUBA1A* expression in a gastric tumor cell line and the inhibitory concentration 50% (IC50) of oxaliplatin *in vitro*.

METHODS

mRNA expression data and patient demographic

Raw expression data and clinical information of patients were downloaded from multi-institutional real world public datasets, including the Gene Expression Omnibus (GEO) dataset (http://www.ncbi.nlm.nih.gov/geo/) [20], the Cancer Genome Atlas (TCGA; https://cancergenome.nih.gov/) [21], and the Gene Expression Profiling Interactive Analysis (GEPIA; http://gepia.cancer-pku.cn/) [22]. In our study, "Gastric cancer vs. Normal Analysis" and "Differential Analysis" were the primary filtering criteria. The following datasets were included in this research: GSE13911 [23], GSE15459 [24], and GSE54129 [25]. The RNA-seq datasets which included *TUBA1A* were used: TCGA [21] and GEPIA [22]. Finally, a total of 1,881 samples, including 1,618 patients with GC and 263 normal samples, were examined.

Immunohistochemical (IHC) staining data of *TUBA1A* protein expression

Protein expression levels of *TUBA1A* were compared between normal and GC tissues using immunohistochemical (IHC) staining data provided by the Human Protein Atlas (HPA; http://www.proteinatlas.org/) [26]. For the acquisition of experimental samples and immunohistochemical methods, specific text instructions and video presentations are provided on the HPA website [26].

IC50 data of oxaliplatin *in vitro*

Primary data of *TUBA1A* in a gastric tumor cell line, and the IC50 of oxaliplatin *in vitro* were downloaded from Genomics of Drug Sensitivity in Cancer (GDSC, https://www.cancerrxgene.org/) [27]. Data pre-processing and statistical analyses were executed with R software 3.5.2.

Single-cell RNA sequencing data

Single-cell RNA sequencing data and results were downloaded from the Mouse Cell Atlas (MCA; http://bis.zju.edu.cn/MCA/index.html) [28]. We investigated *TUBA1A* mRNA expression in different stomach cell types, including more than 13,000 single cells of 17 stomach cell types, by analyzing single-cell RNA sequencing data of the adult mouse stomach. Plots of single-cell *TUBA1A* mRNA expression were drawn using R software 3.5.2.

Gastric cancer methylation data

The possible epigenetic regulation mechanism underlying the dysregulated expression of *TUBA1A* was examined by evaluating methylation data downloaded from the TCGA (TCGA-STAD), including Illumina Human Methylation data. Data pre-processing and statistical analyses were performed with R software 3.5.2.

Data quantification of M0-, M1-, and M2-polarized TAM infiltration in the gastric tumor microenvironment

CIBERSORT [29] was used to calculate the infiltration of M0-, M1-, and M2-polarized TAMs in the gastric tumor immune microenvironment. CIBERSORT is based on the principle of linear support vector regression to deconvolute the expression matrix of human leucocyte subsets [29]; in the current study, the method is based on the known reference set and the gene expression feature set of 22 leukocyte subsets (LM22), including M0-, M1-, and M2-polarized macrophages (LM22 Signature genes file and LM22 Reference sample file, https://cibersort.stanford.edu/download.php). CIBERSORT performed better than other methods and was verified by flow cytometry [29]. We set 100 permutations, using primary data from GSE15459, GSE54129, and TCGA-STAD. Correlations between the expression of *TUBA1A* and the infiltration of M0-, M1-, and M2-polarized TAMs were examined by Pearson correlation test, performed with R software 3.5.2.

Data pre-processing and representation

All samples were defined as either cancer or normal, and the RMA algorithm [30] implemented in R software was applied to normalize datasets, including GSE13911, GSE15459, and

GSE54129. The expression values of *TUBA1A* were the means of all probe sets that included *TUBA1A*. The median value of *TUBA1A* expression was set to a cut-off for high- and low-expression groups.

Statistical analysis

Differences in expression between cancer and normal groups were analyzed by R software using paired and unpaired t-tests with primary data from GSE13911 and GSE54129, respectively. The differences in expression between the cancer and normal groups were analyzed by GEPIA [22] using unpaired t-tests and data from TCGA and the Genotype-Tissue Expression (GTEx, https://gtexportal.org). Correlations between clinicopathological characteristics and *TUBA1A* expression were assessed using chi-squared test with primary data from TCGA and GSE15459. In the current study, the 7th UICC (Union for International Cancer Control) classification of malignant tumors, including stages I–IV, was applied [31]. A stage I tumor, which includes stage IA and stage IB in this system, is considered as early GC [32], whereas tumors of other stages were considered as advanced stages. Higher histologic grade including G3 (grade 3) indicates poorly differentiated carcinoma with poor survival [31].The overall survival, post-progression survival (survival time following progressive disease), and initial progression were assessed using the R package, Kaplan Meier (KM) analysis with log-rank test or the KM plotter (www.kmplot.com) [33]. In addition, unpaired t-tests were applied to analyze differences in expression and methylation between the two groups. The correlation between the expression and methylation of *TUBA1A* was analyzed using Pearson's correlation analysis. A p value < 0.05 was considered statistically significant.

Gene set enrichment analysis

Gene set enrichment analysis (GSEA) was performed to assess whether the discovered sets of genes demonstrated meaningful molecular roles between two biological states [34, 35]. To illuminate the biological roles of *TUBA1A* in GC, we performed enrichment analysis applying the GSEA 3.0, in which gene set permutations were used 1,000 times, and a false discovery rate (FDR) <0.30 and nominal p<0.05 were applied.

In order to avoid the tendentious influence of high *TUBA1A* expression on analysis, we further conducted single sample gene set enrichment analysis (ssGSEA) using a blind method, in which the expression level of *TUBA1A* in each single sample was unknown. ssGSEA can calculate the activity of the specified pathways [36], and in order to analyze the activity of the HDAC pathway, GSK3 pathway, mTOR pathway, and P38MAPK pathway in a single sample, the ssGSEA score was used to quantify the pathway activities using R package GSVA[37] and GSEABase[38]. The stronger the activity of these four pathways, the higher the scores. The ssGSEA scores were normalized by transforming each attribute (the four pathway gene sets) value (ssGSEA score) χ_i into χ_i' by the equation $\chi_i' = (\chi_i - \chi_{min})/(\chi_{max} - \chi_{min})$, where χ_{min} and χ_{max} represent the minimum and maximum of the ssGSEA scores for the gene set across all samples[36], respectively. We hierarchically clustered samples (primary data from GSE15459) on the basis of the normalized ssGSEA scores of the four pathway gene sets, using R package sparcl [39].

RESULTS

***TUBA1A* expression in gastric cancer compared to normal gastric tissues**

Using data from GSE13911, the expression of *TUBA1A* was found to be markedly higher in GC than normal samples (Fig. 1A: 31 GC vs. 31 normal, paired t-tests, p=0.0001). In order to validate these findings and provide further supporting evidence, the GSE54129, TCGA, and GTEx datasets were analyzed. The expression analysis of *TUBA1A* validated the above findings, in that *TUBA1A* expression was markedly higher in GC than in normal samples (Fig. 1B: 111 GC vs. 21 normal, unpaired t-tests, p<0.0001). Furthermore, using data from TCGA and GTEx, the expression of *TUBA1A* was also markedly higher in GC than normal samples (Fig. 1C: 408 GC vs. 211 normal, p<0.01, unpaired *t*-tests, analyzed by GEPIA).

Clinical IHC staining of *TUBA1A* protein expression was compared between normal and GC tissues using IHC staining data provided by the HPA, including 6 normal human samples and 12 GC patients. No staining of *TUBA1A* was detected with anti-*TUBA1A* antibody (CAB008686) in normal gastric tissues (Figs. 1H and 1I), whereas GC tissues mostly exhibited medium intensity of *TUBA1A* staining with the same anti-*TUBA1A* antibody (Figs. 1J and 1K). Statistical analysis was not performed due to the small sample size.

Correlations between expression on *TUBA1A* and overall survival

The expression of *TUBA1A* (n=96 low *TUBA1A* vs. n=96 high *TUBA1A*, primary data from GSE15459) in GC patients was markedly correlated with poor overall survival (log-rank test, χ^2=15.25, p<0.0001; Fig. 1D). The expression levels of *TUBA1A* (n=438 low *TUBA1A* vs. n=438 high *TUBA1A*) in GC patients were markedly correlated with poor overall survival (log-rank test, χ^2=15.82, p<0.0001, by KM plotter; Fig. 1E). In addition, the levels of *TUBA1A* (n=320 low *TUBA1A* vs. n=321 high *TUBA1A*) in GC patients were significantly correlated with first progression (from diagnosed with cancer until first objective cancer progression) (log-rank test, χ^2=14.03, p=0.0002, by KM plotter t; Fig. 1F). The levels of *TUBA1A* (n=250 low *TUBA1A* vs. n=249 high *TUBA1A*) in GC patients were significantly correlated with post-progression survival (log-rank test, χ^2=8.638, p=0.0033, by KM plotter; Fig. 1G). Post-progression survival is survival after progression of cancer. These findings demonstrate that elevated *TUBA1A* is an indicator of poor prognosis in GC.

Correlations between expression on *TUBA1A* and clinicopathological features of gastric cancer patients

Table I summarizes the marked associations between *TUBA1A* expression and the clinicopathological features of GC patients (primary data from GSE15459 and TCGA). *TUBA1A* expression was significantly higher in advanced GC than in early GC. Furthermore, increased *TUBA1A* was markedly correlated with more aggressive pathological subtypes, including invasive subtypes, compared to other subtypes. *TUBA1A*

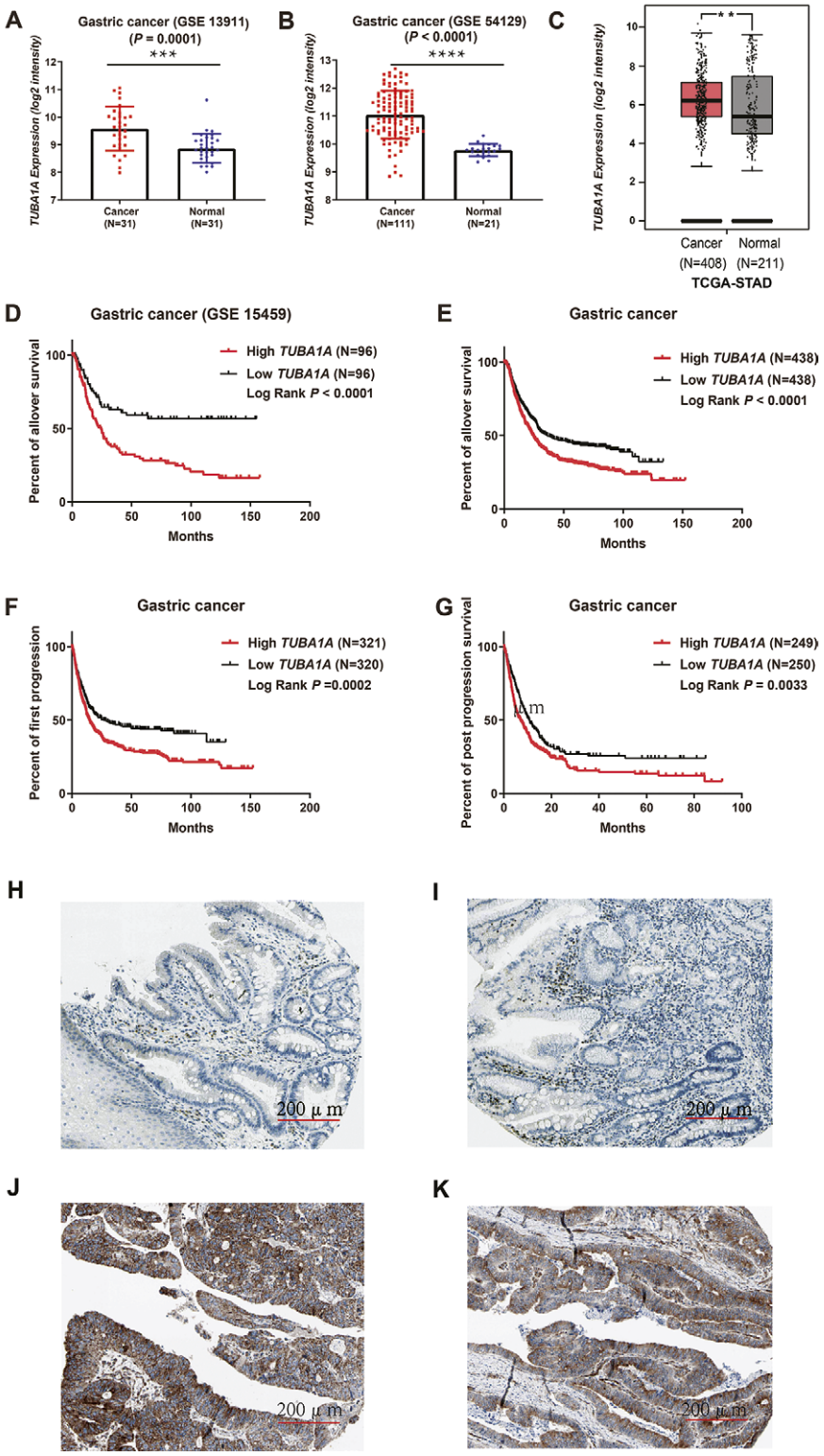

Fig. 1. Expression of *TUBA1A*, and its correlation with prognosis in gastric cancer and the IC50 (inhibitory concentration 50%) of oxaliplatin *in vitro*. A and B) Expression of *TUBA1A* was upregulated in gastric cancer (data from GSE13911, based on paired t-tests; and from GSE54129, based on unpaired t-tests). C) Expression of *TUBA1A* was upregulated in gastric cancer (data from the Cancer Genome Atlas and Genotype-Tissue Expression, based on unpaired t-tests, and analyzed by http://gepia.cancer-pku.cn). The correlation was investigated via Kaplan-Meier analysis and log-rank tests. D) Overall survival of patients with gastric cancer (data from GSE15459). E) Overall survival, F) first progression, and G) post-progression survival of patients with gastric cancer (data from KM plotter, and analyzed by KM plotter) *p < 0.05, **p < 0.01, ***p < 0.001, ****p < 0.0001. H and I) Representative images of IHC TUBA1A staining with anti-TUBA1A antibody (CAB008686) in normal gastric tissues. J and K) Representative images of IHC TUBA1A staining with anti-TUBA1A antibody (CAB008686) in gastric cancer tissues. Data were obtained from the Human Protein Atlas (https://www.proteinatlas.org/ENSG00000167552-TUBA1A/pathology/stomach+cancer#ihc).

expression was significantly elevated in the diffuse type (Lauren classification), compared to its expression in other subtypes of GC.

In addition, elevated *TUBA1A* was significantly correlated with higher histologic grade, including G3 (grade 3).

GSEA results of gastric cancer tissues with high *TUBA1A* expression

To identify *TUBA1A*-related signaling pathways activated in GC, we conducted GSEA between low and high *TUBA1A* expression data sets. Significant differences (FDR<0.30, nominal p-value<0.05) were found, and Fig. 2 show the results of GSEA for GC with high *TUBA1A* expression: HDACPATHWAY [p=0.0039, FDR=0.2251, enrichment score (ES)=0.6460; Fig. 2A); GSK3PATHWAY (p=0.0019, FDR=0.2759, ES=0.6675; Fig. 2B); MTORPATHWAY (p=0.0327, FDR=0.1702, ES=0.5399; Fig. 2C); and P38MAPKPATHWAY (p=0.004, FDR=0.1443, ES=0.5880; Fig. 2D). These findings showed that *TUBA1A* regulated genes related to histone deacetylase (HDAC) pathway, glycogen synthase kinase3 (GSK3) pathway, mammalian target of rapamycin (mTOR) pathway, and P38MAPK pathway in *TUBA1A*-related GC.

Association between pathway activities and *TUBA1A* expression by single sample GSEA analysis

The clustering results showed three subtypes; the heatmap of the three subtypes was plotted (Fig. 2E), and the three clusters were defined as follows: Pathway Activity High (Pathway_Activity_H), Pathway Activity Medium (Pathway_Activity_M), and Pathway Activity Low (Pathway_Activity_L). The expression of *TUBA1A* was analyzed in the three subtypes, and Pathway_Activity_H was found to have the highest *TUBA1A* expression levels, while Pathway_Activity_L had the lowest *TUBA1A* expression levels (ANOVA test, $p < 0.001$) (Fig. 2F). These findings suggested

Table I. Correlations between TUBA1A expression and clinicopathological features of patients with gastric cancer (primary data from GSE15459 and TCGA)

Source of primary data	Characteristic	Cases	TUBA1A expression		χ^2	p
			High	Low		
GSE15459	Age (years)					
	≤ 65	87	49	38	2.5432	0.1108
	> 65	105	47	58		
	Gender					
	Male	125	61	64	0.2063	0.6497
	Female	67	35	32		
	Early vs. advanced GC					
	Early GC	31	10	21	4.6548	0.031*
	Advanced GC	29	86	75		
	Pathological subtype					
	Invasive	51	50	1	72.969	9.871E-16****
	Proliferative	70	21	49		
	Metabolic	40	8	32		
	Unstable	31	17	14		
	Lauren classification					
	Diffuse	75	53	22	22.52	1.288E-05****
	Mixed	18	9	9		
	Intestinal	99	34	65		
TCGA	Age (years)					
	≤ 65	164	88	76	1.4599	0.2269
	> 65	207	98	109		
	Gender					
	Male	241	119	122	0.15408	0.6947
	Female	134	69	65		
	Early vs. advanced GC					
	Early GC	53	15	38	11.7504	0.0006***
	Advance GC	299	161	138		
	Histologic grade					
	G1	10	5	5	15.5758	0.0004***
	G2	137	50	87		
	G3	219	127	92		

Data analyzed by Chi-square tests. *p<0.05; ***p<0.001; ****p<0.0001; GC: gastric cancer

that the higher *TUBA1A* expression samples positively correlate with polarization of macrophages to a greater extent than the lower *TUBA1A* expression samples, since Pathway Activity_H (highest activity of four pathway) was shown to contribute to the polarization of macrophages and enhance the infiltration of M2-polarized TAMs.Taken together,

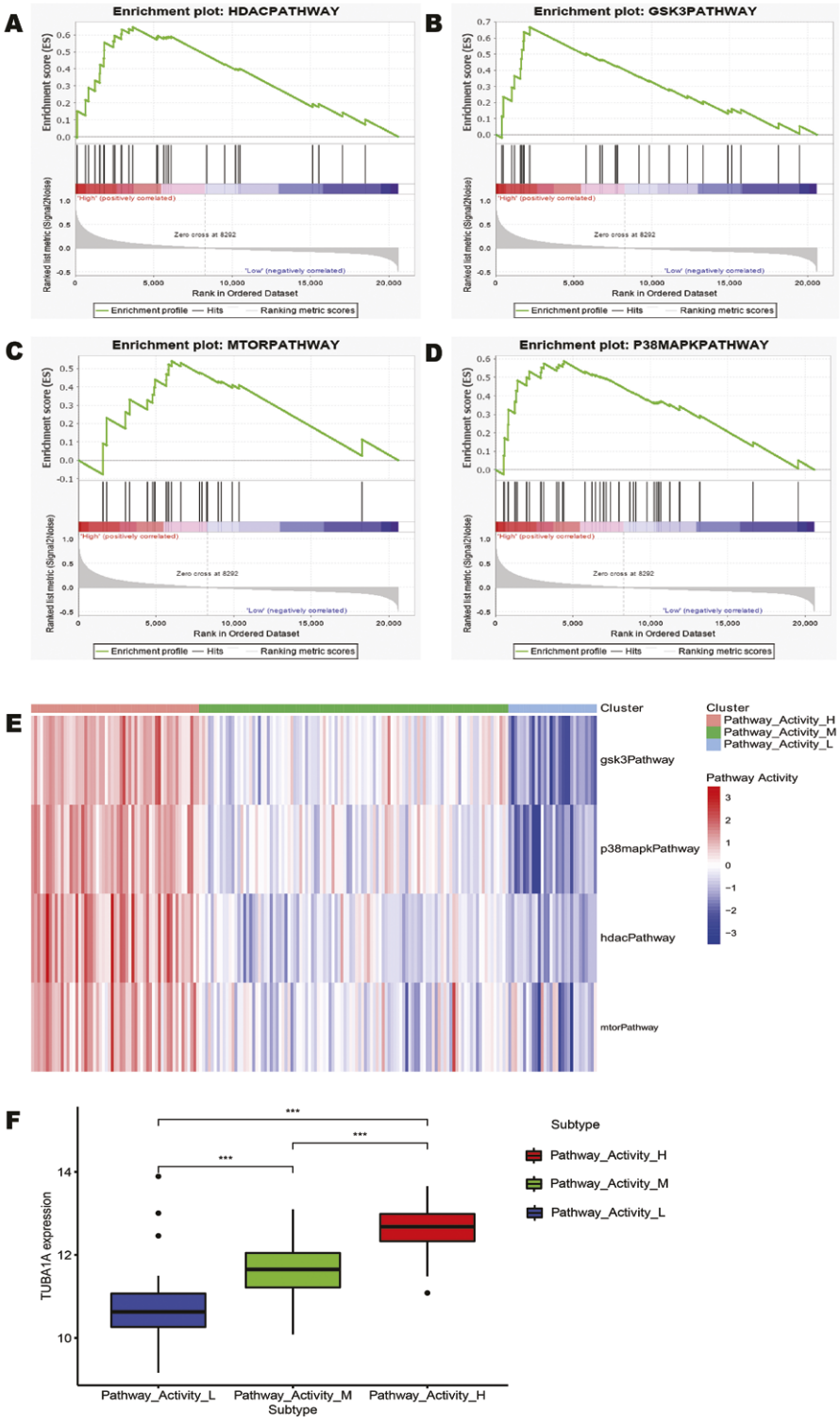

Fig. 2. Gene set enrichment analysis results for gastric cancer tissues with high expression of *TUBA1A*, and association between pathway activity and *TUBA1A* expression by single sample GSEA analysis (data from GSE15459). Gene set enrichment analysis (GSEA) showed that the enriched gene sets were associated with the (A) HDACPATHWAY, (B) GSK3PATHWAY, (C) MTORPATHWAY, and (D) P38MAPKPATHWAY. (E) Heatmap of clustering based on the activity of specified pathways, including the HDAC pathway, GSK3 pathway, mTOR pathway, and the P38MAPK pathway. The three clusters were as follows: Pathway Activity High (Pathway_Activity_H), Pathway Activity Medium (Pathway_Activity_M), and Pathway Activity Low (Pathway_Activity_L). (F) Pathway_Activity_H had the highest TUBA1A expression levels, and Pathway_Activity_L had the lowest TUBA1A expression levels (ANOVA test, $p < 0.001$).

Figs. 2A–D and Figs. 2E–F demonstrate that *TUBA1A* was correlated with macrophage polarization.

Correlation between the expression of *TUBA1A* and the infiltration of tumor-associated macrophages in the gastric tumor immune microenvironment

GSEA revealed that high *TUBA1A* was associated with multiple pathways shown to contribute to the infiltration of M2 TAMs (Fig. 3). Therefore, we analyzed the association between *TUBA1A* expression and infiltration of TAMs, including M0-, M1-, and M2-polarized TAMs, in gastric tumor immune microenvironment, using primary data from GSE15459, GSE54129, and TCGA-STAD. The analyzed results of these datasets are the similarity and mutual verification, which confirmed that the increased infiltration of M2-polarized TAMs was significantly associated with a high expression of *TUBA1A* (Figs. 3D–F, $p < 0.05$, unpaired t-tests). Moreover, a significant positive correlation was found between the level of M2-polarized TAM infiltration and expression of *TUBA1A* using Pearson's correlation analysis (Figs. 3A–C, $p < 0.05$). Furthermore, the infiltration of M1- and M0-polarized TAMs were not significantly associated with *TUBA1A* by unpaired t-tests (Figs. 3J–L and 3P-R, $p > 0.05$), nor was the correlation between the infiltration of M1- and M0-polarized TAMs and the expression of *TUBA1A* by Pearson's correlation (Figs. 3G–I, and 3M–O, $p > 0.05$).

These findings demonstrate that elevated *TUBA1A* contributes to the enhanced infiltration of M2-polarized TAMs in the GC immune microenvironment.

Relationship between *TUBA1A* expression and cytokines involved in TAMs recruitment

In order to confirm the correlation between *TUBA1A* expression and infiltration level of TAMs, we analyzed the relationship between *TUBA1A* expression and cytokines associated with TAM recruitment in GC (primary data from GSE54129 and TCGA-STAD). These cytokines have been implicated in the recruitment of TAMs and M2-macrophages polarization, which include a colony stimulating factor 1 (CSF-1), C-C motif chemokine ligand 2 (CCL2), C-X-C motif chemokine ligand 12(CXCL12), C-X3-C motif chemokine ligand 1 (CX3CL1), and a vascular endothelial growth factor C (VEGFC). The results showed similarity across datasets, in that increased *TUBA1A* expression was found to be significantly associated with high expression levels of CSF-1, CCL2, CXCL12, CX3CL1, and VEGFC (Figure 4A, C, E, G, I, K, M, O, Q, and S, $P < 0.0001–0.001$, unpaired t-tests), and significantly positively correlated with a high expression of CSF-1, CCL2, CXCL12, CX3CL1, and VEGFC by Pearson's correlation test (Figs. 4B, D, F, H, J, L, N, P, R, and T, $p < 0.0001$). As these cytokines promote the recruitment of TAMs and M2-macrophages polarization, these findings further confirm the correlation between *TUBA1A* expression and the infiltration of TAMs.

Elevated expression of *TUBA1A* enhances the IC50 (inhibitory concentration 50%) of oxaliplatin *in vitro*

As *TUBA1A* plays a role in the gastric tumor immune microenvironment, which is continually changing, and M2-polarized TAMs lead to oxaliplatin resistance, we investigated the influence of *TUBA1A* on oxaliplatin by analyzing the correlation between the expression of *TUBA1A* and the IC50 of oxaliplatin *in vitro* (primary data downloaded from https://www.cancerrxgene.org/ and analyzed by R statistic software). We found that elevated *TUBA1A* can affect the IC50 of oxaliplatin *in vitro*, in that an increased IC50 of oxaliplatin was significantly associated with high expression of *TUBA1A* (Fig. 5A, $p < 0.05$, unpaired t-tests). Furthermore, a significant positive correlation was found between the IC50 of oxaliplatin and *TUBA1A* expression by Pearson's correlation analysis (Fig. 5B, $p < 0.05$). A higher IC50 indicates lower inhibitory effects of the drug on tumor cells; thus, the above findings indicate that elevated *TUBA1A* can reduce the inhibitory effect of oxaliplatin on gastric tumor cells.

The expression of *TUBA1A* mRNA in different stomach cell types by analyzing single-cell RNA sequencing data

We further investigated *TUBA1A* mRNA expression in different stomach cell types, including more than 13,000 single cells of 17 stomach cell types, by analyzing single-cell RNA sequencing data of the adult mouse stomach. The results showed that the expression of *TUBA1A* was higher in stomach basal cells, fibroblast cells, and G cells than other stomach cell types (Fig. 5C). Single-cell RNA sequencing data and analysis results were downloaded from the MCA, and plots of single-cell *TUBA1A* mRNA expression were drawn using R software version 3.5.2.

Regulation of *TUBA1A* expression in gastric cancer by methylation

We further investigated the mechanisms underlying the dysregulation of *TUBA1A* by comparing *TUBA1A* expression and methylation levels of methylated sites (primary data from TCGA-STAD). We observed that low methylation levels of methylated sites (cg12441358, cg15367082, cg05692837, and cg21962603) were significantly associated with a high expression of *TUBA1A* by unpaired t-tests (Figs. 6A, C, E, and G, $p<0.05$). A significant correlation was found between *TUBA1A* expression and the methylation level of methylated sites by Pearson's correlation test (Figs. 6B, D, F, and H, $p<0.05$). As fat mass and obesity-associated protein (FTO) has been identified as an important demethylase that can downregulate methylation, we compared the expression of *TUBA1A* and *FTO* (data from GSE15459, GSE54129, and TCGA-STAD). The three datasets showed similar results, in that increased *TUBA1A* expression was significantly associated with high expression levels of *FTO* (Figs. 6I, K, and M, $p<0.0001$, unpaired t-tests), and significantly positively correlated with a high expression of *FTO* by Pearson's correlation test (Figs. 6J, L, and N, $p<0.0001$).

Overall, the above findings confirmed that hypomethylation contributed to the upregulation of *TUBA1A* in stomach cancer.

DISCUSSION

The present study demonstrated that *TUBA1A* was significantly elevated in GC compared to normal gastric tissue. GSEA results revealed that high *TUBA1A* expression was correlated with mTOR and P38MAPK pathways, which mediate changes in cellular signals to control cell proliferation, growth, and survival in tumor cells [40, 41]. An aggressive pathological subtype and poor survival are important

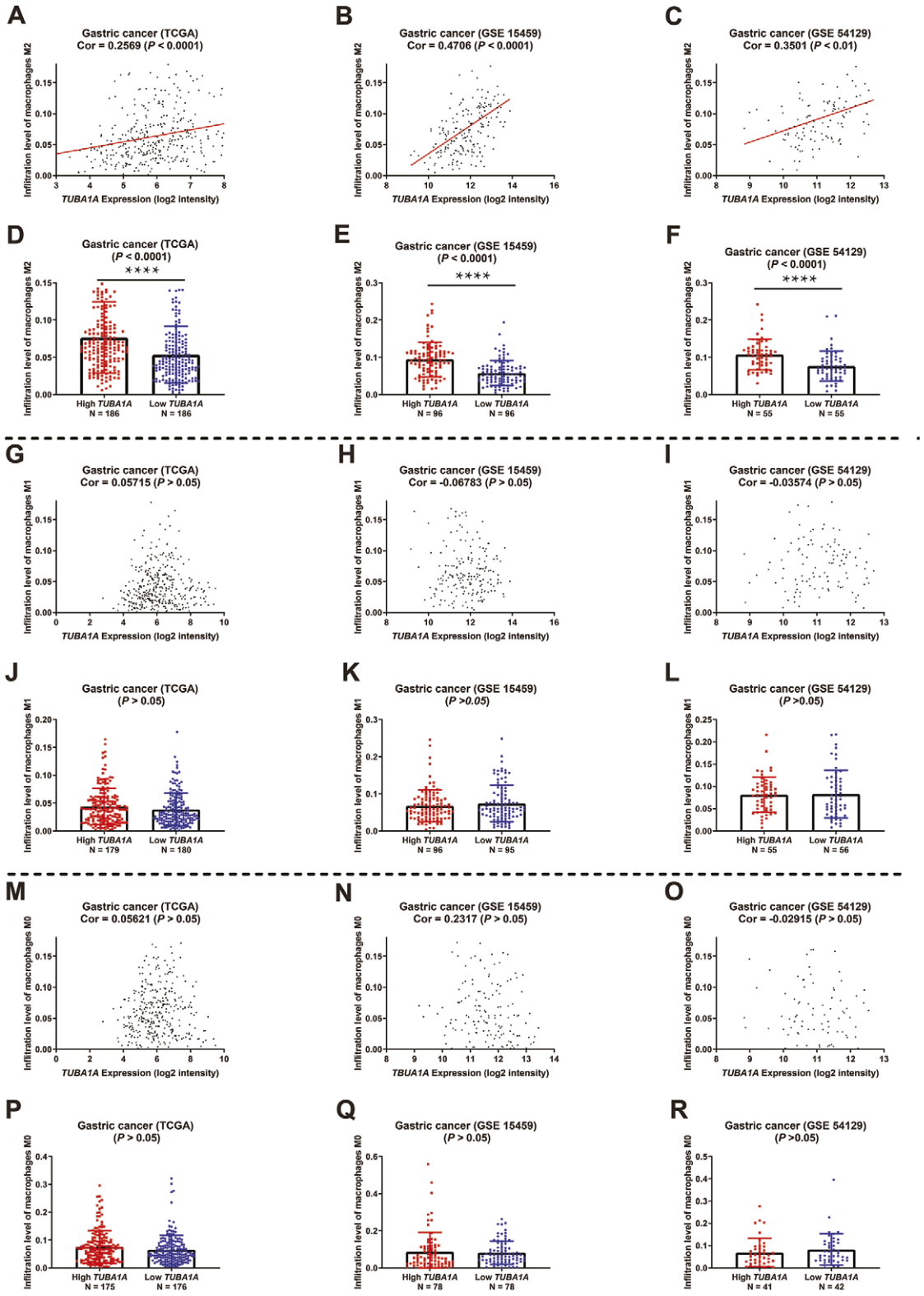

Fig. 3. Correlation between the expression of *TUBA1A* and the infiltration level of M0-, M1-, and M2-polarized macrophages in the gastric tumor microenvironment. (A–C) A significant positive correlation was observed between the infiltration level of M2-polarized TAMs and the expression of *TUBA1A* using Pearson's correlation test. (D–F) Increased infiltration levels of M2-polarized TAMs were significantly associated with high *TUBA1A* expression by unpaired t-tests. (G–I and M–O) No significant correlations were found between the infiltration levels of M0- and M1-polarized TAMs and *TUBA1A* expression by Pearson's correlation test. (J–L and P–R) Infiltration levels of M0- and M1-polarized TAMs were not significantly associated with the expression of *TUBA1A* by unpaired t-tests. (D–F, J–L, and P–R) Patients were divided into high and low groups based on the median value of *TUBA1A* expression at each infiltration level of M2-, M1-, and M0-polarized TAMs. TCGA: The Cancer Genome Atlas, Cor: Pearson's correlation coefficient, TAMs: Tumor-associated macrophages. ****p < 0.0001.

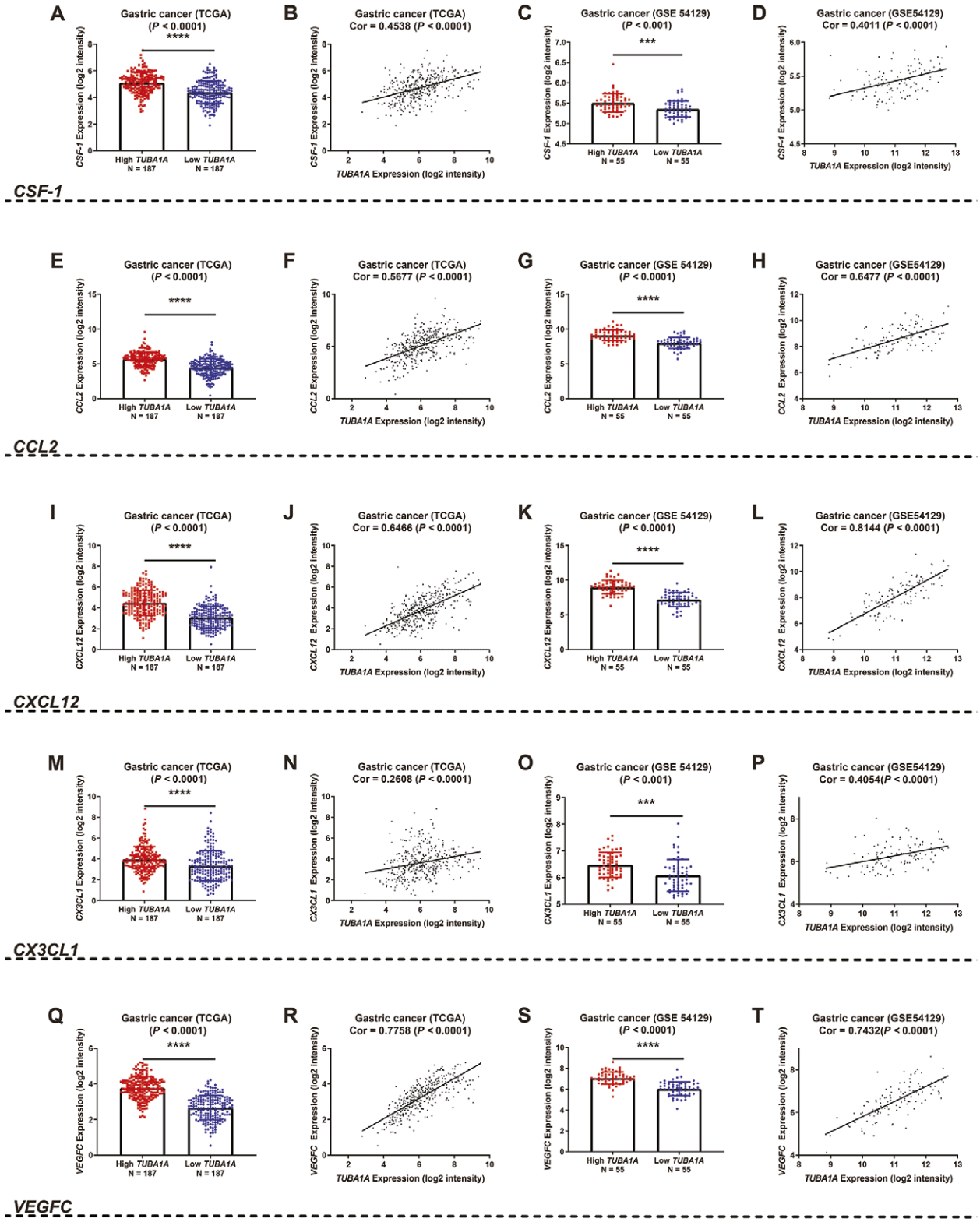

Fig. 4. Relationship between TUBA1A expression and cytokines associated with TAM recruitment. (A, C, E, G, I, K, M, O, Q, and S) Increased TUBA1A expression was significantly associated with high expression of CSF-1, *CCL2, CXCL12, CX3CL1*, and *VEGFC* by unpaired t-tests (***p < 0.001, ****p < 0.0001). Patients were divided into high and low groups based on the median value of *TUBA1A* expression. (B, D, F, H, J, L, N, P, R, and T) Increased *TUBA1A* expression was significantly positively correlated with high expression of *CSF-1, CCL2, CXCL12, CX3CL1*, and *VEGFC* by Pearson's correlation test (p < 0.0001). TCGA: The Cancer Genome Atlas, Cor: Pearson's correlation coefficient, TAMs: Tumor-associated macrophages. ****p < 0.0001.

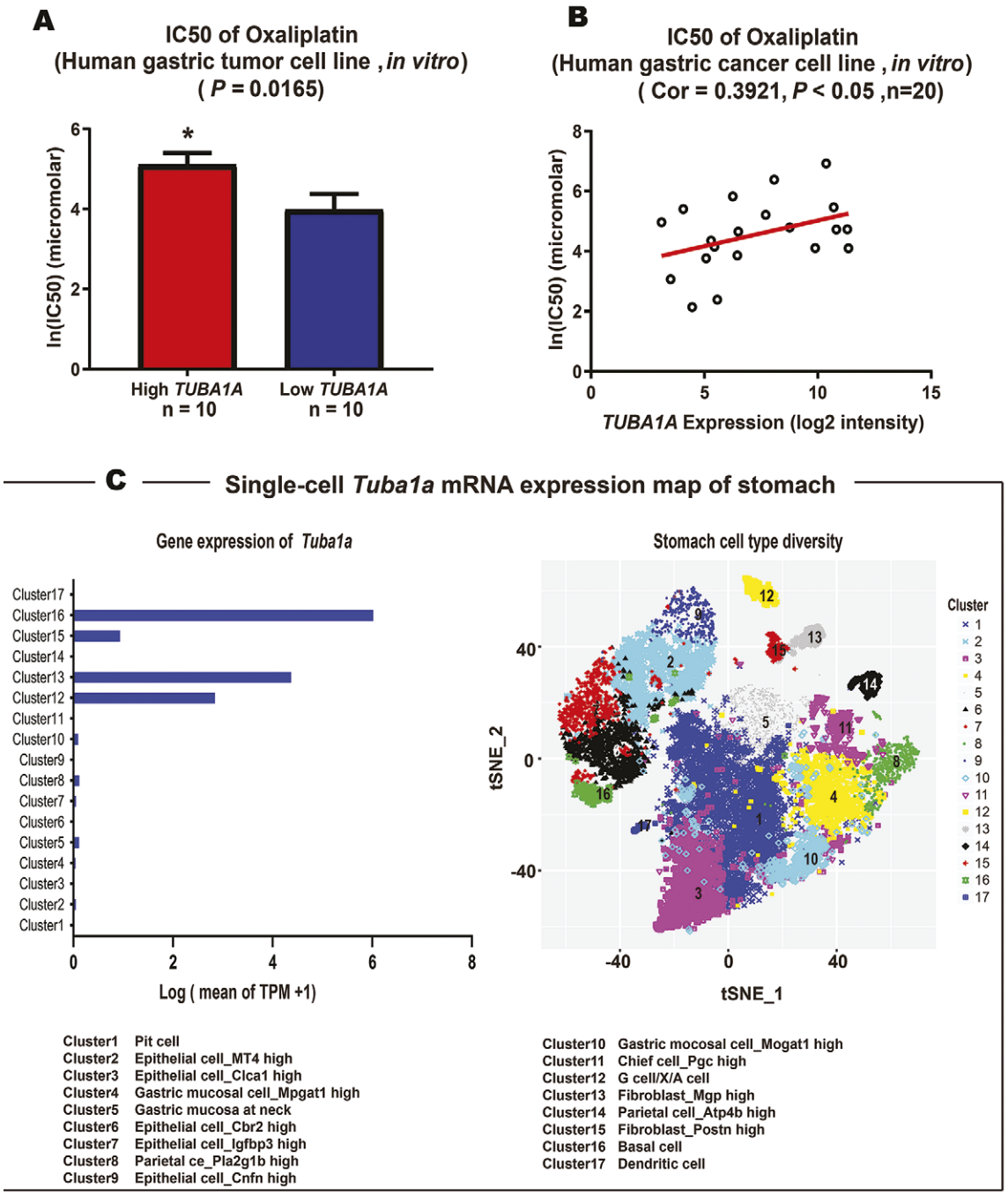

Fig. 5. Correlation between *TUBA1A* expression and the IC50 (inhibitory concentration 50%) of oxaliplatin in vitro, and the single-cell Tuba1a mRNA expression map of adult mouse stomach. (A) An increased IC50 of oxaliplatin was significantly associated with a high expression of *TUBA1A* by unpaired t-tests *p < 0.05. (B) A significant positive correlation was found between the IC50 of oxaliplatin and *TUBA1A* expression by Pearson's correlation analysis. The expression of *TUBA1A* were dichotomized into low- and high-expression groups using the median value as a cu-toff. (C) By analyzing single-cell RNA sequencing data of the adult mouse stomach, which included more than 13000 single cells of 17 stomach cell types, the expression of *Tuba1a* was higher in stomach basal cells, fibroblast cells, and G cells (cluster16, cluster15, cluster13, and cluster12) than other cell types. Plots of single-cell *Tuba1a* mRNA expression were drawn using GraphPad Prism 8 and R software version 3.5.2.

indicators of poor prognosis [32, 42]. In our study, elevated *TUBA1A* expression significantly correlated with poor overall survival, first progression, and post-progression survival.

TUBA1A expression was also markedly increased in invasive pathological subtypes, G3, and advanced GC.

GSEA results revealed that enriched gene sets correlated with HDAC, GSK3, P38MAPK, and mTOR pathways. HDACs can influence the infiltration of pro-tumorigenic M2-macrophages [11], while synergistic activation of the GSK3 and p38MAPK pathways induces M2 polarization of TAMs [43, 44]. M2 polarization of TAMs has been shown to be regulated through the EGFR/PI3K/AKT/mTOR pathway [12]. Targeting M2-polarized TAMs is a novel strategy for cancer treatment [45-47]. As these pathways contribute to the infiltration of M2 tumor-associated macrophages, we hypothesized that *TUBA1A* would also increase the

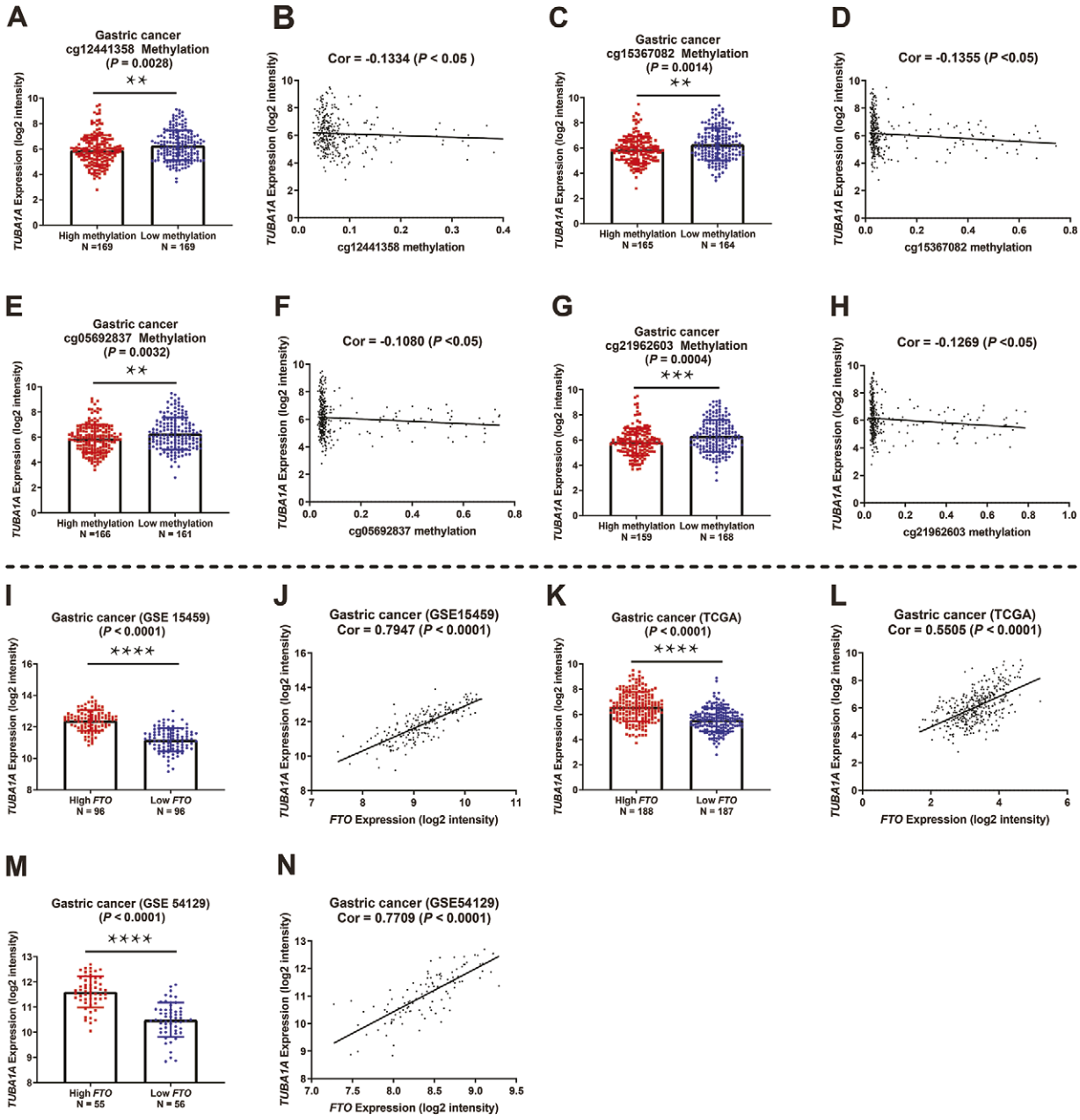

Fig. 6. Expression of TUBA1A is regulated by methylation in gastric cancer. (A, C, E, and G) Low methylation levels of methylated sites (cg12441358, cg15367082, cg05692837, and cg21962603) were significantly associated with high expression levels of TUBA1A by unpaired t-test (data from TCGA). Patients were divided into high and low methylation groups based on the median value for each methylated site probe (cg12441358, cg15367082, cg05692837, and cg21962603) (data from TCGA). (B, D, F, and H) A significantly negative correlation was found between TUBA1A expression and the methylation level of methylated sites (cg12441358, cg15367082, cg05692837, and cg21962603) by Pearson's correlation test (data from TCGA). (I, K, and M) Increased expression of TUBA1A was significantly associated with high expression of FTO by the unpaired t-test. Patients were divided into high and low methylation groups based on the median value of FTO expression. (J, L, and N) Increased expression of TUBA1A was significantly positively associated with high expression levels of FTO by Pearson's correlation test. TCGA: The Cancer Genome Atlas, Cor: Pearson's correlation coefficient. **p < 0.01, ***p < 0.001, ****p < 0.0001.

infiltration of M2-polarized macrophages. This was confirmed in our study, as an increased infiltration of M2-polarized TAMs was significantly associated with a high expression of *TUBA1A* (Figs. 3D–F), with a significant positive correlation found between the infiltration level of M2-polarized TAMs and *TUBA1A* expression (Figs. 3A–C). Some cytokines have been implicated in the recruitment of TAMs and M2-macrophages polarization, including CSF-1 [48, 49], CCL2 [50, 51], CXCL12 [52], CX3CL1 [53], and VEGFC [54, 55]. Our results showed that increased *TUBA1A* expression was significantly positively correlated with a high expression of CSF-1, CCL2, CXCL12, CX3CL1, and VEGFC. These findings further confirm the correlation between *TUBA1A* expression and the infiltration of TAMs. These results were generated from three real-world datasets, which showed similarity and mutual verification.

Oxaliplatin is used in the treatment of GC [15-17]; however, changes in tumor microenvironment, especially related to TAMs, could lead to fa ailure of oxaliplatin therapy [9, 18, 19]. We examined the influence of *TUBA1A* on oxaliplatin by analyzing the correlation between *TUBA1A* expression and IC50 of oxaliplatin *in vitro*. Higher IC50 indicates lower inhibitory effects of the drug on tumor cells, and we found that high *TUBA1A* expression significantly increased IC50 of oxaliplatin *in vitro*, which suggests elevated *TUBA1A* can reduce the inhibitory effect of oxaliplatin on gastric tumor cells.

Single-cell RNA sequencing data, which included more than 13,000 single cells, demonstrated that *TUBA1A* was higher in stomach fibroblast cells, basal cells, and G cells than other stomach cell types. Tumor cell/fibroblast co-culture can induce M2-polarization of TAMs [56]. Fibroblast-induced M2-polarized macrophages have been shown to significantly increase cancer cell growth, invasion, and migration [57]. Our results indicated that *TUBA1A* might enhance M2-polarized macrophage infiltration by influencing fibroblasts, G cells that synthesize gastrin, as well as in basal cells [58]. These findings provide new clues to the synthesis of gastrin and function of basal cells.

Epigenetic regulation, including histone modifications and methylation, is a vital mechanism of dysregulated genes in cancer, with lower methylation exhibiting significantly higher gene expression [59, 60]. We found that lower DNA methylation exhibited significantly higher *TUBA1A* expression, indicating that epigenetic alterations contribute to the upregulation of *TUBA1A*. Furthermore, elevated *TUBA1A* expression was positively associated with high levels of FTO, which can downregulate methylation as an important demethylase [61]. These findings indicate that hypomethylation contributes to the upregulation of *TUBA1A* in GC.

CONCLUSIONS

The present study revealed that the expression of *TUBA1A* was higher in GC and was an indicator of poor prognosis. High *TUBA1A* might contribute to tumorigenesis and enhance the infiltration level of M2-polarized macrophages in the gastric tumor immune microenvironment. Furthermore, high *TUBA1A* expression increased the IC50 of oxaliplatin *in vitro*, and the increase in *TUBA1A* was shown to be mediated by hypomethylation.

Conflicts of interest: None to declare.

Authors' contribution: D.W. conceived and designed the study. Z.J., Y.J. and S.Z. collected the data. D.W. analysed the data. D.W. wrote the manuscript. All authors read the manuscript and agreed to the final version.

REFERENCES

1. Gardner JF, Cushion TD, Niotakis G, et al. Clinical and Functional Characterization of the Recurrent TUBA1A p.(Arg2His) Mutation. Brain Sci 2018;8:145. doi:10.3390/brainsci8080145
2. Keays DA, Tian G, Poirier K, et al. Mutations in alpha-tubulin cause abnormal neuronal migration in mice and lissencephaly in humans. Cell 2007;128:45-57. doi:10.1016/j.cell.2006.12.017
3. Hebebrand M, Hüffmeier U, Trollmann R, et al. The mutational and phenotypic spectrum of TUBA1A-associated tubulinopathy. Orphanet J Rare Dis 2019;14:38. doi:10.1186/s13023-019-1020-x
4. Horbach L, Sinigaglia M, Da Silva CA, et al. Gene expression changes associated with chemotherapy resistance in Ewing sarcoma cells. Mol Clin Oncol 2018;8:719-724. doi:10.3892/mco.2018.1608
5. Mandelkow E, Mandelkow EM. Microtubules and microtubule-associated proteins. Curr Opin Cell Biol 1995;7:72-81. doi:10.1016/0955-0674(95)80047-6
6. Nami B, Wang Z. Genetics and Expression Profile of the Tubulin Gene Superfamily in Breast Cancer Subtypes and Its Relation to Taxane Resistance. Cancers (Basel) 2018;10:274. doi:10.3390/cancers10080274
7. Zhang L, Li S. Lactic acid promotes macrophage polarization through MCT-HIF1α signaling in gastric cancer. Exp Cell Res 2020;388:111846. doi:10.1016/j.yexcr.2020.111846
8. Kumar V, Donthireddy L, Marvel D, et al. Cancer-Associated Fibroblasts Neutralize the Anti-tumor Effect of CSF1 Receptor Blockade by Inducing PMN-MDSC Infiltration of Tumors. Cancer Cell 2017;32:654-668.e5. doi:10.1016/j.ccell.2017.10.005
9. Noy R, Pollard JW. Tumor-associated macrophages: from mechanisms to therapy. Immunity 2014;41:49-61. doi:10.1016/j.immuni.2014.06.010
10. Rey-Giraud F, Hafner M, Ries CH. In vitro generation of monocyte-derived macrophages under serum-free conditions improves their tumor promoting functions. PLoS One 2012;7:e42656. doi:10.1371/journal.pone.0042656
11. Knox T, Sahakian E, Banik D, et al. Selective HDAC6 inhibitors improve anti-PD-1 immune checkpoint blockade therapy by decreasing the anti-inflammatory phenotype of macrophages and down-regulation of immunosuppressive proteins in tumor cells. Sci Rep 2019;9:6136. doi:10.1038/s41598-019-42237-3
12. Lian G, Chen S, Ouyang M, Li F, Chen L, Yang J. Colon Cancer Cell Secretes EGF to Promote M2 Polarization of TAM Through EGFR/PI3K/AKT/mTOR Pathway. Technol Cancer Res Treat 2019;18:1533033819849068. doi:10.1177/1533033819849068
13. Wang X, Luo G, Zhang K, et al. Hypoxic Tumor-Derived Exosomal miR-301a Mediates M2 Macrophage Polarization via PTEN/PI3Kγ to Promote Pancreatic Cancer Metastasis. Cancer Res 2018;78:4586-4598. doi:10.1158/0008-5472.CAN-17-3841
14. Weigert A, Tzieply N, von Knethen A, et al. Tumor cell apoptosis polarizes macrophages role of sphingosine-1-phosphate. Mol Biol Cell 2007;18:3810-3819. doi:10.1091/mbc.e06-12-1096
15. Sato Y, Kurokawa Y, Doki Y, et al. A Phase II study of preoperative chemotherapy with docetaxel, oxaliplatin and S-1 in gastric cancer with extensive lymph node metastasis (JCOG1704). Future Oncol 2020;16:31-38. doi:10.2217/fon-2019-0528
16. Xu R, He X, Wufuli R, et al. Choice of Capecitabine or S1 in Combination with Oxaliplatin based on Thymidine Phosphorylase and Dihydropyrimidine Dehydrogenase Expression Status in Patients with Advanced Gastric Cancer. J Gastric Cancer 2019;19:408-416. doi:10.5230/jgc.2019.19.e40
17. Yoshikawa T, Muro K, Shitara K, et al. Effect of First-line S-1 Plus Oxaliplatin With or Without Ramucirumab Followed by Paclitaxel Plus Ramucirumab on Advanced Gastric Cancer in East Asia: The Phase 2 RAINSTORM Randomized Clinical Trial. JAMA Netw Open 2019;2:e198243. doi:10.1001/jamanetworkopen.2019.8243

18. Fu XT, Song K, Zhou J, et al. Tumor-associated macrophages modulate resistance to oxaliplatin via inducing autophagy in hepatocellular carcinoma. Cancer Cell Int 2019;19:71. doi:10.1186/s12935-019-0771-8
19. Ruffell B, Coussens LM. Macrophages and therapeutic resistance in cancer. Cancer Cell 2015;27:462-472. doi:10.1016/j.ccell.2015.02.015
20. Barrett T, Edgar R. Mining microarray data at NCBI's Gene Expression Omnibus (GEO)*. Methods Mol Biol 2006;338:175-190. doi:10.1385/1-59745-097-9:175
21. Hutter C, Zenklusen JC. The Cancer Genome Atlas: Creating Lasting Value beyond Its Data. Cell 2018;173:283-285. doi:10.1016/j.cell.2018.03.042
22. Tang Z, Li C, Kang B, Gao G, Li C, Zhang Z. GEPIA: a web server for cancer and normal gene expression profiling and interactive analyses. Nucleic Acids Res 2017;45:W98-W102. doi:10.1093/nar/gkx247
23. D'Errico M, de Rinaldis E, Blasi MF, et al. Genome-wide expression profile of sporadic gastric cancers with microsatellite instability. Eur J Cancer 2009;45:461-469. doi:10.1016/j.ejca.2008.10.032
24. Ooi CH, Ivanova T, Wu J, et al. Oncogenic pathway combinations predict clinical prognosis in gastric cancer. PLoS Genet 2009;5:e1000676. doi:10.1371/journal.pgen.1000676
25. Yang L, Wang J, Li J, et al. Identification of Serum Biomarkers for Gastric Cancer Diagnosis Using a Human Proteome Microarray. Mol Cell Proteomics 2016;15:614-623. doi:10.1074/mcp.M115.051250
26. Uhlén M, Björling E, Agaton C, et al. A human protein atlas for normal and cancer tissues based on antibody proteomics. Mol Cell Proteomics 2005;4:1920-1932. doi:10.1074/mcp.M500279-MCP200
27. Yang W, Soares J, Greninger P, et al. Genomics of Drug Sensitivity in Cancer (GDSC): a resource for therapeutic biomarker discovery in cancer cells. Nucleic Acids Res 2013;41:D955-D961. doi:10.1093/nar/gks1111
28. Han X, Wang R, Zhou Y, et al. Mapping the Mouse Cell Atlas by Microwell-Seq. Cell 2018;172:1091-1107.e17. doi:10.1016/j.cell.2018.02.001
29. Newman AM, Liu CL, Green MR, et al. Robust enumeration of cell subsets from tissue expression profiles. Nat Methods 2015;12:453-457. doi:10.1038/nmeth.3337
30. Irizarry RA, Hobbs B, Collin F, et al. Exploration, normalization, and summaries of high density oligonucleotide array probe level data. Biostatistics 2003;4:249-264. doi:10.1093/biostatistics/4.2.249
31. Sobin LH, Gospodarowicz MK, Wittekind C. (eds.). TNM classification of malignant tumours. 7th ed. Oxford. Wiley-Blackwell; 2009.
32. Bollschweiler E, Berlth F, Baltin C, Mönig S, Hölscher AH. Treatment of early gastric cancer in the Western World. World J Gastroenterol 2014;20:5672-5678. doi:10.3748/wjg.v20.i19.5672
33. Szász AM, Lánczky A, Nagy Á, et al. Cross-validation of survival associated biomarkers in gastric cancer using transcriptomic data of 1,065 patients. Oncotarget 2016;7:49322-49333. doi:10.18632/oncotarget.10337
34. Subramanian A, Tamayo P, Mootha VK, et al. Gene set enrichment analysis: a knowledge-based approach for interpreting genome-wide expression profiles. Proc Natl Acad Sci U S A 2005;102:15545-15550. doi:10.1073/pnas.0506580102
35. Zheng F, Yu H, Lu J. High expression of MUC20 drives tumorigenesis and predicts poor survival in endometrial cancer. J Cell Biochem 2019;120:11859-11866. doi:10.1002/jcb.28466
36. He Y, Jiang Z, Chen C, Wang X. Classification of triple-negative breast cancers based on Immunogenomic profiling. J Exp Clin Cancer Res 2018;37:327. doi:10.1186/s13046-018-1002-1
37. Hänzelmann S, Castelo R, Guinney J. GSVA: gene set variation analysis for microarray and RNA-seq data. BMC Bioinformatics 2013;14:7. doi:10.1186/1471-2105-14-7
38. Morgan M, Falcon S, Gentleman R. GSEABase: Gene set enrichment data structures and methods. Available at: https://rdrr.io/bioc/GSEABase/
39. Witten DM, Tibshirani R. sparcl: Perform Sparse Hierarchical Clustering and Sparse K-Means Clustering. Avilable at: https://rdrr.io/cran/sparcl/
40. Tjomsland V, Bojmar L, Sandström P, et al. IL-1α expression in pancreatic ductal adenocarcinoma affects the tumor cell migration and is regulated by the p38MAPK signaling pathway. PLoS One 2013;8:e70874. doi:10.1371/journal.pone.0070874
41. Zhang N, Lu C, Chen L. miR-217 regulates tumor growth and apoptosis by targeting the MAPK signaling pathway in colorectal cancer. Oncol Lett 2016;12:4589-4597. doi:10.3892/ol.2016.5249
42. Carter CL, Allen C, Henson DE. Relation of tumor size, lymph node status, and survival in 24,740 breast cancer cases. Cancer 1989;63:181-187. doi:10.1002/1097-0142(19890101)63:1<181::aid-cncr2820630129>3.0.co;2-h
43. Park SH, Park-Min KH, Chen J, Hu X, Ivashkiv LB. Tumor necrosis factor induces GSK3 kinase-mediated cross-tolerance to endotoxin in macrophages. Nat Immunol 2011;12:607-615. doi:10.1038/ni.2043
44. Schmieder A, Schledzewski K, Michel J, et al. Synergistic activation by p38MAPK and glucocorticoid signaling mediates induction of M2-like tumor-associated macrophages expressing the novel CD20 homolog MS4A8A. Int J Cancer 2011;129:122-132. doi:10.1002/ijc.25657
45. Komohara Y, Jinushi M, Takeya M. Clinical significance of macrophage heterogeneity in human malignant tumors. Cancer Sci 2014;105:1-8. doi:10.1111/cas.12314
46. Cieslewicz M, Tang J, Yu JL, et al. Targeted delivery of proapoptotic peptides to tumor-associated macrophages improves survival. Proc Natl Acad Sci U S A 2013;110:15919-15924. doi:10.1073/pnas.1312197110
47. Vadevoo SMP, Kim JE, Gunassekaran GR, et al. IL4 Receptor-Targeted Proapoptotic Peptide Blocks Tumor Growth and Metastasis by Enhancing Antitumor Immunity. Mol Cancer Ther 2017;16:2803-2816. doi:10.1158/1535-7163.MCT-17-0339
48. Wang H, Shao Q, Sun J, et al. Interactions between colon cancer cells and tumor-infiltrated macrophages depending on cancer cell-derived colony stimulating factor 1. Oncoimmunology 2016;5:e1122157. doi:10.1080/2162402X.2015.1122157
49. Braza MS, Conde P, Garcia M, et al. Neutrophil derived CSF1 induces macrophage polarization and promotes transplantation tolerance. Am J Transplant 2018;18:1247-1255. doi:10.1111/ajt.14645
50. Ding M, He SJ, Yang J. MCP-1/CCL2 Mediated by Autocrine Loop of PDGF-BB Promotes Invasion of Lung Cancer Cell by Recruitment of Macrophages Via CCL2-CCR2 Axis. J Interferon Cytokine Res 2019;39:224-232. doi:10.1089/jir.2018.0113
51. Li X, Yao W, Yuan Y, et al. Targeting of tumour-infiltrating macrophages via CCL2/CCR2 signalling as a therapeutic strategy against hepatocellular carcinoma. Gut 2017;66:157-167. doi:10.1136/gutjnl-2015-310514
52. Beider K, Bitner H, Leiba M, et al. Multiple myeloma cells recruit tumor-supportive macrophages through the CXCR4/CXCL12 axis and promote their polarization toward the M2 phenotype. Oncotarget 2014;5:11283-11296. doi:10.18632/oncotarget.2207
53. Ishida Y, Kuninaka Y, Yamamoto Y, et al. Pivotal Involvement of the CX3CL1-CX3CR1 Axis for the Recruitment of M2 Tumor-Associated

Macrophages in Skin Carcinogenesis. J Invest Dermatol 2020;140:1951-1961.e6. doi:10.1016/j.jid.2020.02.023

54. Skobe M, Hamberg LM, Hawighorst T, et al. Concurrent induction of lymphangiogenesis, angiogenesis, and macrophage recruitment by vascular endothelial growth factor-C in melanoma. Am J Pathol 2001;159:893-903. doi:10.1016/S0002-9440(10)61765-8
55. D'Alessio S, Correale C, Tacconi C, et al. VEGF-C-dependent stimulation of lymphatic function ameliorates experimental inflammatory bowel disease. J Clin Invest 2014;124:3863-3878. doi:10.1172/JCI72189
56. Kuen J, Darowski D, Kluge T, Majety M. Pancreatic cancer cell/fibroblast co-culture induces M2 like macrophages that influence therapeutic response in a 3D model. PLoS One 2017;12:e0182039. doi:10.1371/journal.pone.0182039
57. Zhang A, Qian Y, Ye Z, et al. Cancer-associated fibroblasts promote M2 polarization of macrophages in pancreatic ductal adenocarcinoma. Cancer Med 2017;6:463-470. doi:10.1002/cam4.993
58. Smith JP, Nadella S, Osborne N. Gastrin and Gastric Cancer. Cell Mol Gastroenterol Hepatol 2017;4:75-83. doi:10.1016/j.jcmgh.2017.03.004
59. Asadollahi R, Hyde CA, Zhong XY. Epigenetics of ovarian cancer: from the lab to the clinic. Gynecol Oncol 2010;118:81-87. doi:10.1016/j.ygyno.2010.03.015
60. Kwon MJ, Shin YK. Epigenetic regulation of cancer-associated genes in ovarian cancer. Int J Mol Sci 2011;12:983-1008. doi:10.3390/ijms12020983
61. Chen J, Du B. Novel positioning from obesity to cancer: FTO, an m6A RNA demethylase, regulates tumour progression. J Cancer Res Clin Oncol 2019;145:19-29. doi:10.1007/s00432-018-2796-0